

ORIGINAL
ARTICLE

Identification and quantification of blood–brain barrier transporters in isolated rat brain microvessels

Hajar Al Feteisi*¹,  Zubida M. Al-Majdoub*¹, Brahim Achour*, Narciso Couto†, Amin Rostami-Hodjegan*·‡ and Jill Barber*

*Centre for Applied Pharmacokinetic Research (CAPKR), University of Manchester, Manchester, UK

†ChELSI Institute, Department of Chemical and Biological Engineering, University of Sheffield,

Sheffield, UK

‡Simcyp Limited (a Certara Company), Sheffield, UK

Abstract

The blood–brain barrier (BBB) maintains brain homeostasis by tightly regulating the exchange of molecules with systemic circulation. It consists primarily of microvascular endothelial cells surrounded by astrocytic endfeet, pericytes, and microglia. Understanding the make-up of transporters in rat BBB is essential to the translation of pharmacological and toxicological observations into humans. In this study, experimental workflows are presented in which the optimization of (a) isolation of rat brain microvessels (b) enrichment of endothelial cells, and (c) extraction and digestion of proteins were evaluated, followed by identification and quantification of BBB proteins. Optimization of microvessel isolation was indicated by 15-fold enrichment of endothelial cell marker Glut1 mRNA, whereas markers for other cell types were not enriched. Filter-aided sample preparation was shown to be superior to in-solution sample preparation (10251 peptides vs. 7533 peptides). Label-free proteomics was used to identify nearly 2000 proteins and

quantify 1276 proteins in isolated microvessels. A combination of targeted and global proteomics was adopted to measure protein abundance of 6 ATP-binding cassette and 27 solute carrier transporters. Data analysis using proprietary Progenesis and open access MaxQuant software showed overall agreement; however, Abcb9 and Slc22a8 were quantified only by MaxQuant, whereas Abcc9 and Abcd3 were quantified only by Progenesis. Agreement between targeted and untargeted quantification was demonstrated for Abcb1 (19.7 ± 1.4 vs. 17.8 ± 2.3) and Abcc4 (2.2 ± 0.7 vs. 2.1 ± 0.4), respectively. Rigorous quantification of BBB proteins, as reported in this study, should assist with translational modeling efforts involving brain disposition of xenobiotics.

Keywords: blood–brain barrier, label-free quantification, methodology optimization, QconCAT, rat brain microvessels, transporters.

J. Neurochem. (2018) **146**, 670–685.

Guidelines for developmental, behavioral, chemical, and neurotoxicity testing of new therapeutic entities have been adopted by the Food and Drug Administration (Sobotka *et al.* 1996). Pre-clinical studies depend upon the use of animal models, and rodents represent the main animals used in mainstream neuroscience and neurotoxicity research; in 2015, about 32% of publications in neuroscience research used rodents (Keifer and Summers 2016). Typically, rodents are short-lived, making them a valuable model in aging studies, where measurement over the lifetime of the same rodent is an attractive option. Rodents have been successfully used in studies of certain human neurological diseases (Persidsky *et al.* 2006; Erickson and

Received December 26, 2017; revised manuscript received March 26, 2018; accepted April 5, 2018.

Address correspondence and reprint requests to Dr Jill Barber, Centre for Applied Pharmacokinetic Research (CAPKR), University of Manchester, Stopford Building, Oxford Road, Manchester M13 9PT, UK. E-mail: jill.barber@manchester.ac.uk

¹These authors contributed equally to this work.

Abbreviations used: ABC, ATP-binding cassette; BBB, blood–brain barrier; BCA, bichinchoninic acid; BSA, bovine serum albumin; CNS, central nervous system; CSF, cerebrospinal fluid; DDI, drug–drug interaction; FASP, filter-aided sample preparation; IVIVE, *in vitro-in vivo* extrapolation; LC–MS/MS, liquid chromatography–tandem mass spectrometry; NNOP, non-naturally occurring peptide; PBPK, physiologically based pharmacokinetics; QconCAT, quantification concatemer; SLC, solute carrier; TransCAT, transporters QconCAT.

Banks 2013) as well as studies of brain transport and metabolism (Cardoso *et al.* 2010; Uchida *et al.* 2014). However, it is important that inter-species differences are taken into consideration in the translation of findings to human biology, especially when *in vitro-in vivo* extrapolation using physiologically based pharmacokinetic (PBPK) modeling is implemented.

The concepts of model-based translation of animal observations into human consequences were recently described by our group in two different contexts, nephrotoxicity (Scotcher *et al.* 2016) and fetal exposure and developmental safety (Abduljalil *et al.* 2018). In summary, these involve considerations of 'local exposure' in a specific organ in animal and linking these parameters to toxicological or pharmacological effects in humans after consideration of anatomical, physiological, and biological differences, particularly in relation to the type and abundance of xenobiotic transporters. This ensures that classical extrapolation of the dose–effect relationship does not lead to erroneous conclusions when there are disparities in dose–local exposure ratios between species. Such strategies are depicted schematically in Fig. 1.

The blood–brain barrier (BBB) consists primarily of microvessel endothelial cells. These cells are supported by the basal lamina and surrounded by astrocytic endfeet and pericytes, packed between astrocytes and endothelial cells. Microglia tend to be in close proximity to these cellular structures, and along with pericytes and nerve terminals, they play key roles in induction, maintenance, and function

of the BBB (Abbott *et al.* 2006, 2010). The BBB has an important role in brain homeostasis by tightly regulating the exchange of molecules between the brain and systemic circulation, although small and lipophilic molecules easily diffuse through the BBB. Characterization of BBB transporters is vital to understanding the disposition of molecules between the blood and the brain interstitial fluid. Carrier-mediated transport allows access of nutrients (such as glucose and amino acids) to brain interstitial fluid, and receptor-mediated transport facilitates uptake of larger molecules, including insulin, leptin, and iron transferrin (Pardridge *et al.* 1985). Brain endothelial cells also efflux certain substances back into the blood (Zheng *et al.* 2003). ATP-binding cassette (ABC) and solute carrier (SLC) transporters are the main transporters expressed in the BBB. ABC transporters include P-glycoprotein (Abcb1/Mdr1), breast cancer resistance protein (Abcg2/Bcrp), and multidrug resistance-associated proteins (Abcc/Mrp) (Dauchy *et al.* 2008; Uchida *et al.* 2011). These transporters are localized at the luminal membrane and efflux their substrates into the blood circulation by energy-dependent, unidirectional, outwardly directed transport (Schinkel and Jonker 2012). SLC transporters can be responsible for uptake, disposition, and efflux; important members of this class are the Slc22 subfamily (Oat, Oct, and Octn) and Slco transporters (Golden and Pollack 2003). The physiology of brain transporters has previously been reviewed in detail (Giacomini *et al.* 2010).

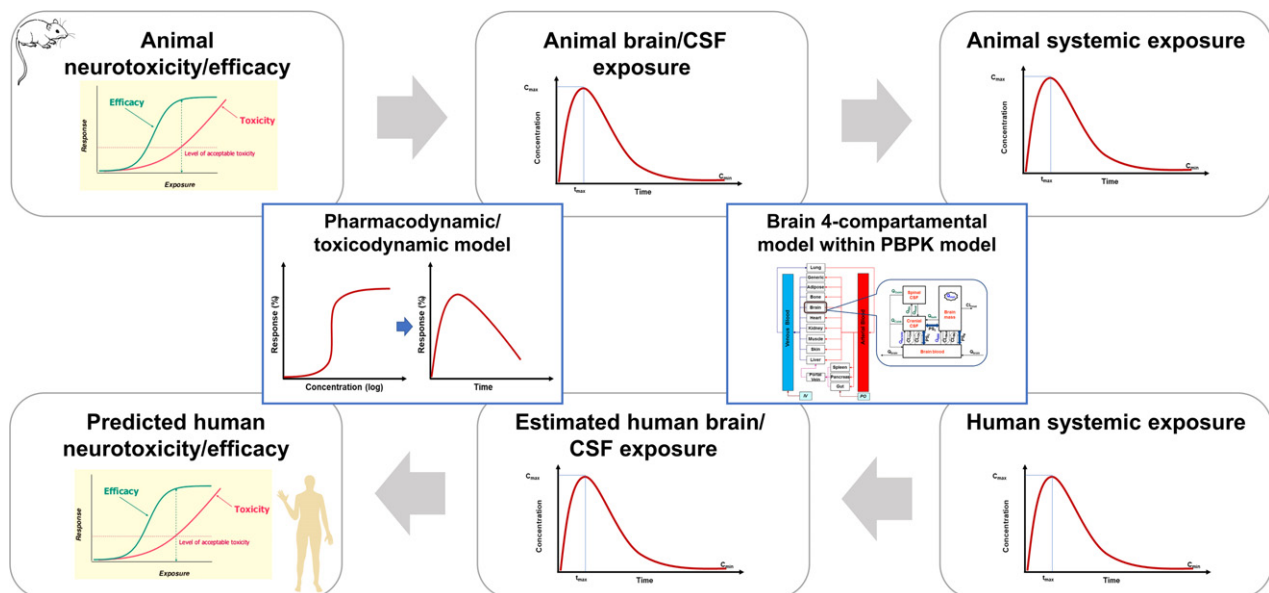


Fig. 1 Prediction of pharmacological efficacy and neurotoxicity using brain physiologically based pharmacokinetic (PBPK) modeling in the translation from pre-clinical efficacy/neurotoxicity studies; a pharmacodynamic/toxicodynamic model is used to create response–exposure relationships that connect pre-clinical efficacy/neurotoxicity studies to systemic exposure. A brain PBPK model is used to assess systemic

exposure and predict human brain tissue concentration by taking into account parameters affected by species differences (CSF flow rate, CSF volume, weight, brain transporters abundances). Estimated human brain tissue exposure can be further used to predict pharmacological response or toxicity when species differences are considered in the pharmacodynamic/toxicodynamic model.

The aim of the work described here was to quantify the abundance of transporters in rat BBB. This is important because the use of rat as a pre-clinical test model, for translation into human medicine, requires such abundance data, which are scarcely available in the literature. In this report, we describe a systematic approach to the optimization of isolation of rat brain microvessels and subsequent quantification of BBB transporters using proteomic and transcriptomic methods. Isolating microvessels from brain cortical tissue is challenging owing to loss and contamination with other cell types; our methods were based on those of Yousif *et al.* (2007) but were adapted for use with frozen rather than fresh tissue. For the first time, the degree of enrichment and purity of the isolated microvessels was assessed using a combination of RNA and protein expression of specific gene markers of endothelial cells (Glu1), pericytes (Cspg4), neurons (Syp), and astrocytes (Gfap). The optimization involved a comparison of two sample preparation methodologies and two data analysis tools. Furthermore, we defined the integrity of replicate measurements by a novel method. Finally, the abundance of endogenous and drug transporters in isolated microvessels was quantified using a proteomic strategy incorporating untargeted label-free measurement with targeted quantification concatemer (QconCAT) (Silva *et al.* 2006; Achour *et al.* 2015).

Materials and methods

Materials and reagents

Materials and chemicals were purchased from Sigma-Aldrich (Poole, UK) unless otherwise indicated. The unlabeled non-naturally occurring peptide calibrator [Glu¹]-Fibrinopeptide B (EGVNDNEEGFFSAR, purity 95%) was purchased from Severn Biotech (Worcestershire, UK). Lysyl endopeptidase (Lys-C) was purchased from Wako (Osaka, Japan). CComplete Mini, EDTA-free protease inhibitor cocktail and recombinant proteomic-grade trypsin were supplied by Roche Applied Sciences (Mannheim, Germany). The QconCAT (TransCAT) was produced in-house as previously described (Russell *et al.* 2013). Bicinchoninic acid protein assay kit was purchased from Pierce (Rockford, IL, USA). RNeasy Micro Kit was purchased from QIAGEN (Hilden, Germany). High Capacity cDNA RT Kit, TaqMan Fast Universal PCR Master Mix, and TaqMan Gene Expression Assay were purchased from Applied Biosystems (Foster City, CA, USA). Solvents used in this study were of HPLC grade (Thermo Fisher, Waltham, MA, USA).

Animals

Adult male Sprague–Dawley rat (Charles River, Kent, UK) brains were a gift from the Centre for Applied Pharmacokinetic Research (University of Manchester) and were by-products of the generation of *in vitro* hepatocyte models under institutional approval (license number 1001/S1). Animals had been maintained according to institutional guidelines, in a temperature-controlled environment with free access to food and water, and were killed at 6–7 weeks of age. The study was not pre-registered and not blinded. Randomization and sample size calculation were not

performed. Rat brain cortex was freshly isolated within 30 min of death followed by freezing with liquid nitrogen and storage at -80°C until use to prepare microvessels.

Tissue preparation and isolation of rat brain microvessels

Frozen rat brain samples were thawed on ice and four pools of 3–4 brains each were prepared (average weight = 3 grams). Once thawed, all subsequent steps were performed on ice. Brain cortex was finely minced and homogenized using 10 up-and-down non-rotated strokes in a hand-held homogenizer in Buffer 1 (8 g/L NaCl, 400 mg/L KCl, 185.4 mg/L $\text{CaCl}_2 \cdot 2\text{H}_2\text{O}$, 60 mg/L KH_2PO_4 , 200 mg/L $\text{MgSO}_4 \cdot 7\text{H}_2\text{O}$, 350 mg/L NaHCO_3 , 1 g/L D-glucose, 90 mg/L $\text{Na}_2\text{HPO}_4 \cdot 7\text{H}_2\text{O}$, 2.4 mg/L HEPES, pH 7.4) using volumes of 4–5 mL/g tissue in a 50 mL tube. Four different isolations were prepared in this study (nominally labeled 1–4; Fig. 2). Protease inhibitor was added to the homogenate to prevent proteolytic degradation in subsequent sample preparation. The homogenates were centrifuged at 2000 g for 10 min at 4°C . The resulting pellet was suspended in 16% dextran and subsequently centrifuged at 5500 g for 15 min at 4°C . The supernatant was transferred to a fresh tube and centrifuged again in a similar way before suspending the two pellets in 10 mL of Buffer 2 (Buffer 1 containing 5 mg/mL bovine serum albumin). The suspension was then passed through a 100 μm nylon mesh and 10 mL Buffer 2 was used to rinse the tube and mesh of residual homogenate (total volume should be <20 mL). The retained part that passed through the mesh was then passed through a 20 μm nylon mesh, and <20 mL Buffer 2 was used to rinse the tube and mesh of residual homogenate. The fraction retained on the filter was transferred to microcentrifuge tubes and centrifuged at 1000 g for 5 min at 4°C . The pellet was then dissolved in 1 mL Buffer 2 and further centrifuged at 1000 g for 5 min at 4°C . Finally, the resultant microvessel pellet was stored in 1 mL isotonic buffer (1 M Tris-HCl, 10 mM NaCl, 1.5 mM MgCl_2 , pH 7.4) at -80°C until further analysis.

RNA extraction and qRT-PCR

To assess the purity and enrichment of isolated microvessels, RNA extraction from rat brain homogenates and corresponding microvessels, and quantitative RT-PCR of cell marker genes were carried out as described in Appendix S1. The cell types and their corresponding marker genes were: endothelial cells (Glu1/Slc2a1), pericytes (Cspg4), astrocytes (Gfap), and neurons (Syp). Transporter gene expression (Abcb1a, Abcg2, and Abcc4) was also quantified in isolated microvessels.

Sample preparation of brain microvessel isolates for proteomic analysis

Protein content was determined for all isolates using a bicinchoninic acid assay. Three pools of rat brain microvessel isolates (1–3) were prepared in-solution (labeled 1S, 2S, and 3S) in duplicate as described previously (Harwood *et al.* 2015; Masuda *et al.* 2008). One replicate of sample 3 (labeled 3F) and two replicates of sample 4 (labeled 4F) were prepared using filter-aided sample preparation (FASP) (Wiśniewski *et al.* 2009). A QconCAT standard (TransCAT) (Russell *et al.* 2013) was used for targeted quantification in sample 4F. Details of the two sample preparation protocols and peptide desalting are included in Appendix S1.

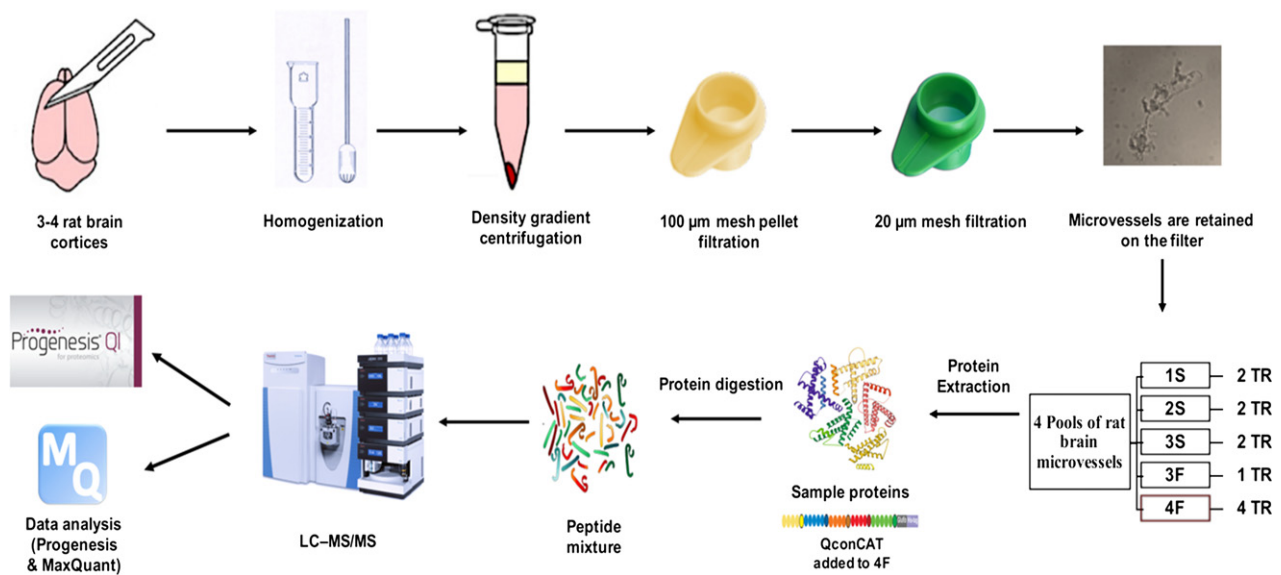


Fig. 2 Experimental workflow of the isolation, identification, and quantification of rat brain microvessel proteins using targeted and untargeted proteomic strategies; S, in-solution sample preparation; F, filter-aided sample preparation; TR, technical replicates.

Liquid chromatography–mass spectrometry (LC–MS/MS) analysis

Desalted samples were resuspended in 10 µL of loading buffer [5% acetonitrile in 0.1% formic acid (FA)] and 1 µL was loaded onto an UltiMate® 3000 (Dionex, Surrey, UK) liquid chromatography system coupled to an on-line Q Exactive™ HF Hybrid Quadrupole-Orbitrap™ mass spectrometer (Thermo Fisher, Bremen, Germany). For samples 1S, 2S, 3S, and 3F, peptides were reversed-phase separated on PepMap™ RSLC C18 column (100 Å, 50 cm × 75 µm i.d., 2 µm particle size) preceded by a C₁₈ PepMap™ 100 µ-Precolumn (100 Å, 5 mm × 5 µm i.d., 5 µm) (Thermo Scientific, Waltham, Massachusetts, United States). A multi-step gradient was used from 4% Buffer B (80% acetonitrile, 0.1% FA) and 96% Buffer A (0.1% FA in HPLC water) to 40% Buffer B over 100 min at a flow rate of 300 nL/min. Peptides from sample 4F were separated using a multi-step gradient from 95% Buffer A (0.1% FA in HPLC water) and 5% Buffer B (0.1% FA in acetonitrile) to 7% B at 1 min, 18% B at 58 min, 27% B at 72 min, and 60% B at 75 min, at a flow rate of 300 nL/min, on a 75 mm × 250 µm i.d., 1.7 µm CSH C₁₈ analytical column (Waters, Milford, MA, UK).

The Q Exactive mass spectrometer acquired data in a data-dependent manner alternating between full-scan MS and MS/MS scans. The following acquisition parameters were used for positive ionization mode: a spray voltage of 2.1 kV and capillary temperature of 250°C. MS scans were acquired over 100–1500 *m/z*, with 60 000 resolution, automatic gain control of 3×10^6 , and 100 ms maximal injection time. Selected precursor ions, top 12, were sequentially fragmented by higher energy collisional dissociation with 28–34% normalized collision energy, isolated window was set to 1.2 *m/z*. These MS/MS scans were acquired at 30 000 resolution, automatic gain control of 5×10^4 and 120 ms maximal injection time. Dynamic exclusion was set to 30 s. Each sample was run in two technical replicates (except

sample 3F) and sample 4 was run in two analytical replicates for each technical replicate (Fig. 2).

Data analysis and protein quantification

Proteins were identified against UniProtKB database using Mascot search engine (<http://www.matrixscience.com/>). QconCAT-based quantification was carried out as previously described (Achour *et al.* 2014; Harwood *et al.* 2015) to measure the abundance of Atp1a1, Abcb1, and Abcc4. Untargeted data analysis and label-free quantification were performed on MaxQuant version 1.5.5.1 (Max Planck Institute of Biochemistry, Martinsried, Germany) and Progenesis QI (Nonlinear Dynamics, Newcastle upon Tyne, UK) using QconCAT-based abundance of Atp1a1 as a reference, and further confirmed using Abcb1. Abundance measurement of ABC and SLC transporters used a combination of targeted and untargeted proteomic methods (Al Feteisi *et al.* 2015a; Achour *et al.* 2017). Details of data analysis and quantification approaches are provided in Appendix S1.

Percentage identical peptides and percentage identical proteins

Percentage identical peptides (PIP) was calculated as follows:

$$\text{PIP} = \frac{\text{Number of common peptides in replicates}}{\text{Number of peptides in either or both replicates}} \times 100\%$$

All peptides considered had a rank of 1 and a Mascot score of at least 15.

A razor was applied to the data. The use of more than one database and the presence of fragment proteins in the database required this step. The number of times each peptide appeared in the worksheet was calculated. Starting from the top of the worksheet, where a protein had no peptides unique to the worksheet, it was removed and the remainder recalculated.

Table 1 Summary of the main steps considered in optimizing tissue and sample preparation

Optimization step	Rationale	Conditions
Addition of protease inhibitor cocktail to the homogenate during microvessel isolation	Protease inhibitors prevent proteolytic degradation of microvessel proteins	According to manufacturer's recommendations
Optimization of the centrifugation speed and concentration of dextran solution	The type of centrifuge and nature of sample (fresh or frozen) affect the quality of isolation; dextran concentration in the gradient centrifugation step helps separate microvessels, which are heavier, from the myelin layer	Centrifuge: swinging bucket rotor; speed: 5500 <i>g</i> ; dextran at 14–18%
Substituting gauze filters with sieving device (cell strainer)	Faster and easier handling than gauze filtration, enabling aseptic handling and easier collection of retained microvessels by reversing on the tube and flushing	
Use of low-binding plastic material and BSA in isolation Buffer 2	BSA is used to reduce adsorption of microvessels to the surfaces of tubes and pipette tips	BSA is added to Buffer 2 at 5 mg/mL
Use of solubilizing agent	Detergents allow for efficient protein solubilization/digestion	10% sodium deoxycholate
Use of a chaotropic agent	The chaotropic agent disrupts the integrity of the cell and facilitates protein solubilization	8 M Urea

BSA, bovine serum albumin.

Fragment proteins and proteins derived from cDNA were removed preferentially, followed by small proteins. The final datasheet contained only proteins with at least one peptide unique to the database and to this sheet.

The percentage identical proteins (PIPr) were then calculated in the same way as PIP.

Subcellular localization and functional analysis

PANTHER (Protein ANalysis THrough Evolutionary Relationships) classification system version 12.0 (<http://www.pantherdb.org/>) was used for bioinformatics analysis of all identified proteins to assign protein class and molecular function (Mi *et al.* 2013). Protein data annotation for subcellular localization was done by database search against UniProtKB (<http://www.uniprot.org/>) and the Gene Ontology Project (<http://geneontology.org/>).

Statistical data analysis

Data were expressed as mean \pm SD of three replicates for gene expression and four replicates for protein abundance (sample 4F). Statistical difference between mean values was determined by unpaired *t*-test using GraphPad Prism version 7.0b for Mac (GraphPad Software, San Diego, CA, USA).

Results

Isolation of rat brain microvessels

Four rat brain microvessel samples (1–4) were prepared from pools of 3–4 brain cortices. Microscopic inspection was performed during isolation to evaluate isolation quality (microvessels were of roughly equal size and showed defined structures). Protein content of the microvessel samples was (mean \pm SD): (1) 108 \pm 18, (2) 202 \pm 02, (3) 295 \pm 12, and (4) 247 \pm 10 μ g protein per gram brain. These

concentrations represent uncorrected values of the scaling factor: brain microvessels protein per gram brain (BMvPGB). Optimization of microvessel isolation needed to be considered to achieve better yield as shown in Table 1.

Assessment of the isolation quality of brain microvessels

Visual inspection with light microscopy did not distinguish brain endothelial cells from pericytes or astrocytes. Consequently, mRNA quantification was implemented with sample 4 to further assess the quality of the isolation through the assessment of marker genes specific to the neurovascular unit cells. The relative mRNA expression of marker genes of endothelial cells, pericytes, astrocytes, and neurons (Glut1, Cspg4, Gfap, and Syp, respectively) were measured using quantitative PCR in isolated microvessels relative to corresponding brain cortex homogenates (Fig. 3a). Glucose transporter (Glut1) relative expression showed significant enrichment (15-fold) of endothelial cells in microvessels compared to brain cortex homogenate ($p < 0.0001$). Microvessel purity was ascertained using relative expression of Cspg4, Gfap, and Syp. Gfap and Syp expression showed a significant decrease in microvessels ($p < 0.05$ and < 0.0001 , respectively), whereas Cspg4 expression showed no statistical difference between isolated microvessels and homogenates.

Transporter gene expression in brain microvessels

Expression of plasma membrane marker (Atp1a1) and transporters (Abcb1a, Abcg2, Abcc4) in isolated microvessels was normalized to endothelial marker (Glut1) (Fig. 3b). Expression of these transporters in isolated microvessels indicates localized expression in brain microvessels in relation to their

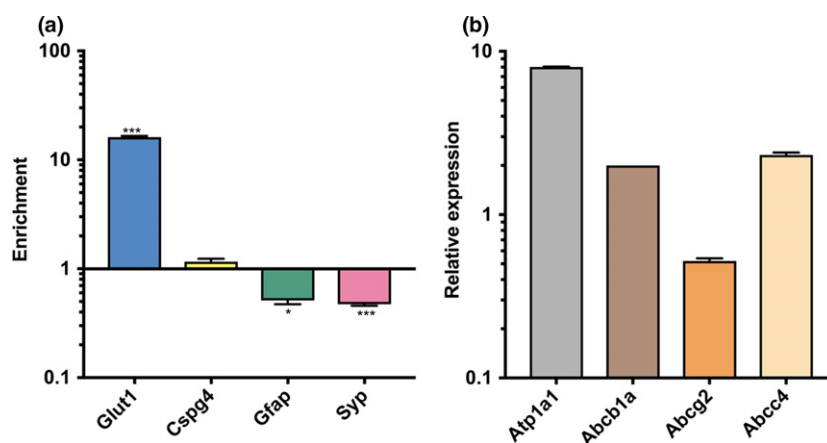


Fig. 3 RNA expression of marker and target genes; (a) enrichment of endothelial cells (Glut1), pericytes (Cspg4), astrocytes (Gfap), and neurons (Syp) in isolated microvessels compared to cortex homogenates; (b) relative gene expressions of membrane marker (Atp1a1) and drug transporter genes (Abcb1a, Abcg2, Abcc4) in isolated microvessels relative to endothelial marker gene (Slc2a1/

Glut1); the data represent mean values \pm SD (number of rat brain used = 4 rat brains per pool; number of replicates = 3 technical replicates, were used to generate gene expression from rat brain microvessels and homogenates), * p < 0.05, ** p < 0.01, *** p < 0.001 for isolated microvessels compared to cortex homogenates using unpaired t -test.

function. Abcb1a mRNA level (2.01 ± 0.003) was higher than Abcg2 (0.52 ± 0.02) which is in a similar order to data reported in the literature (Hoshi *et al.* 2013). However, Abcc4 showed higher expression (2.32 ± 0.08) than Abcb1a and Abcg2, indicating differences in rank order between RNA and protein expression. Abcb1b expression was assessed in these samples but was not determined, indicating little expression of this gene in rat BBB.

Optimization of sample preparation

Comparison of two sample preparation methods was carried out in terms of the number of peptides and transporters identified in four pools of rat brain microvessels. Isolated microvessel samples (1S, 2S, 3S) were prepared in-solution (S) and samples (3F, 4F) were prepared using FASP (F). The progress in the optimization of sample preparation can be observed in the increase in the number of peptides identified by LC-MS/MS in the samples processed using FASP compared to those prepared using in-solution sample preparation (Fig. 4a). At the peptide level, analysis of samples (3F, 4F) identified more than 10 000 peptides (using MaxQuant), while samples (1S, 2S, 3S) showed fewer than 8000 peptides.

The number of ABC transporters identified was the highest in sample 4F (Fig. 4b). Samples prepared using FASP identified more SLC transporter in general when compared to samples prepared in-solution (less than 40 proteins).

Two technical replicates of sample 4F (4F1 and 4F2) were assessed and two different aliquots of each were analyzed by LC-MS/MS. The aliquots were of different protein amounts

(4F1a, 4F2a = $0.67 \mu\text{g}$ and 4F1b, 4F2b = $2.0 \mu\text{g}$) as shown in Fig. 4(c). Although some peptides were identified in the more dilute sample that did not appear in the more concentrated sample, overall the higher amount increased the number of peptides identified by approximately 2500.

Protein identification

With the conditions for sample preparation established, two different software packages (MaxQuant and Progenesis) were evaluated. In the best replicate (4F1b), MaxQuant identified 10041 peptides, Progenesis 8846. Of these, 7782 (70.1%) were identified by both packages (Tables S1 and S2). The reason behind this difference might be the different types of profile data used (continuum vs. centroid). Progenesis uses continuum spectra imported from the mass spectrometer, in which the entire peak profile is stored and analyzed, which means more information available than centroid files imported into MaxQuant. This extra information allows Progenesis to accurately remove background noise, leading to cleaner data. Therefore, this is expected to identify fewer peptides with more accurate identification and quantitation. We therefore continued to use Progenesis for the identification of proteins, but manually assessed both sets of data for the more tractable set of transporter proteins (Table 2).

Percentage identical peptides and percentage identical proteins

LC-MS/MS detects peptides as the primary analyte, but in any experiment, only a small proportion of the available peptides are, in practice, detected. Some of the factors that

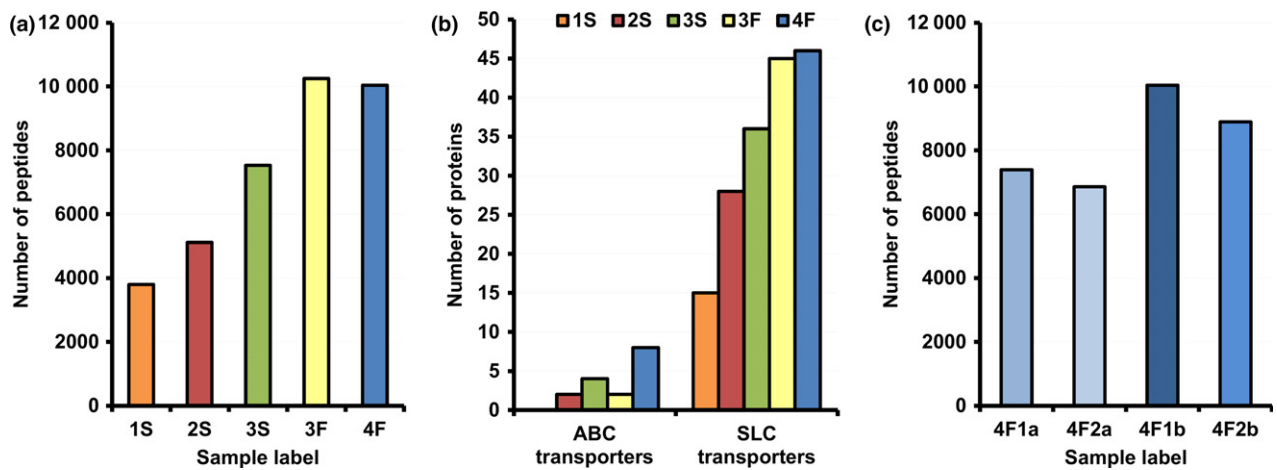


Fig. 4 Method optimization and assessment using proteomic data; (a, b) comparison between in-solution (S) and filter-aided (F) sample preparation methods in terms of the number of peptides and transporters identified in four pools of rat brain microvessels ($n = 4$, samples 1–4), respectively. Samples 1S, 2S, and 3S were prepared in-solution (S), samples 3F and 4F were prepared using filter-aided

sample preparation (F). (a) The numbers of peptides identified in four samples; (b) the numbers of transporters identified in four samples; and (c) the numbers of peptides identified in two technical replicates of sample 4F (1,2) where different amounts of sample were analyzed as analytical replicates (a,b) ($a = 0.67 \mu\text{g}$, $b = 2.0 \mu\text{g}$). In panels (a) and (c), MaxQuant was used to analyze the LC-MS/MS data.

determine whether a peptide is detected have been explored for MALDI and electrospray mass spectrometry (Couto *et al.* 2011, unpublished), and the position of the basic residue and the hydrophobicity of the peptide are important. Variations in performance of the instrumentation and in the preparation of samples can lead to different peptides being detected. In this case, technical replicates gave rise to the detection of 72% or 67% identical peptides (using Progenesis) depending upon the amount of analyte used. The corresponding numbers were a little lower with MaxQuant (66% and 61%) (Table S1). We believe these values to be satisfactory.

The initial output from Progenesis included many duplicate entries because two databases were used. A razor was applied within Excel until each protein remaining contained at least one peptide unique to the datasheet (Table S3). The PIPr could now be calculated and was found to be 89% or 83%, again depending upon the amount of analyte, suggesting that the experimental conditions employed were highly reproducible (Table S1). A summary of the proteins identified and quantified is provided in Tables S4 and S5, respectively.

Subcellular localization and function of identified microvessel proteins

Proteins identified (1980 in total) were annotated for subcellular location, molecular function, and protein class by analyzing accession numbers or gene names against UniProtKB and PANTHER databases (Fig. 5). Based on these results, the main cellular locations of identified proteins were assigned to the cytoplasm (19%), plasma membrane (18%) and the nucleus (14%) (Fig. 5b). In addition, the

highest number of proteins had catalytic or binding function (33%, 36%). Transport activity represented 9.8% of all proteins (Fig. 5a), with this number expected to be higher due to limitations in the extraction of these membrane-bound proteins. Figure 5(c) shows assignment of proteins based on protein class, in which the majority of proteins were classified as nucleic acid binding proteins (217 proteins), cytoskeletal proteins (142 proteins), hydrolases (142 proteins), enzyme modulators (140 proteins), and transporters (98 proteins).

Identification and quantification of rat BBB transporters

The strategy used in this study allowed identification of 8 ABC and 44 SLC transporters (Table S6), of which 10 were identified at the protein level in rat brain for the first time (Table 3). Assessment of the abundance of 26 proteins (transporters, markers, and receptors) in isolated microvessels from rat brain cortices is shown in Table 2 and Fig. 6. QconCAT-derived standard peptides (Russell *et al.* 2013) were used to quantify three proteins (Atp1a1, Abcb1, Abcc4) using one peptide each (the original QconCAT was designed to specifically target human liver transporters). In Table 2, additional proteins were quantified by label-free analysis based on the plasma membrane marker, Atp1a1, as a reference for normalization of data generated using two proteomic data analysis software packages (MaxQuant and Progenesis). A second reference protein, Abcb1 was then used to confirm the results. The label-free analysis was able to generate abundances similar to targeted quantification (Figure S1) and in line with literature (Hoshi *et al.* 2013). The limit of quantification was estimated as previously

Table 2 Abundances of markers, transporters, and receptors in isolated Sprague–Dawley rat brain microvessels

Protein/transporter	Protein expression (mean ± SD) [fmol/μg]					Literature values Rat ^c
	Targeted (QconCAT)	Label-free (untargeted) quantification ^a				
		Progenesis		MaxQuant		
		Reference (Abcb1)	Reference (Atp1a1)	Reference (Abcb1)	Reference (Atp1a1)	
Plasma membrane marker						
Atp1a1	26.19 ± 1.22 ^d	26.51 ± 2.79	–	26.27 ± 6.03	–	68.60 ± 4.5 ^d
Atp1b1		53.58 ± 9.67	44.67 ± 7.99	31.85 ± 10.93	30.88 ± 2.28	
ABC transporters						
Abcb1 (Mdr1, P-gp)	19.65 ± 1.35	–	16.23 ± 1.18	–	17.81 ± 2.33	19.00 ± 2.00
Abcc4 (Mrp4)	2.16 ± 0.74	1.51 ± 0.23	1.53 ± 0.15	1.89 ± 0.74	2.06 ± 0.39	1.60 ± 0.29
Abcg2 (Bcrp)		2.66 ± 0.18	2.76 ± 0.17	3.74 ± 0.20	3.39 ± 0.75	4.15 ± 0.29
Abcb9		11.70 ± 2.42	12.75 ± 4.09			
Abcd3				1.70 ± 0.06	1.34 ± 0.21	
Abcc9 (Mrp9)				0.50 ± 0.17	0.59 ± 0.03	
SLC transporters						
Slc2a1 (Glut1)		93.14 ± 13.65	94.11 ± 7.67	73.73 ± 9.21	72.91 ± 1.85	84.00 ± 4.10
Slc7a5 (Lat1)		2.68 ± 0.37	3.15 ± 0.81	4.28 ± 1.88	4.25 ± 0.97	3.41 ± 0.74
Slco1a4 (Oatp1a4)		1.54 ± 0.33	1.49 ± 0.09	1.47 ± 0.14	1.06 ± 0.11	
Slc4a1 (Ae1)		7.68 ± 0.86	7.05 ± 1.90	7.18 ± 1.78	5.71 ± 0.57	
Slc25a5 (Ant2)		19.81 ± 5.55	18.31 ± 1.06	20.95 ± 4.13	23.30 ± 2.07	
Slc16a1 (Mct1)		6.50 ± 1.81	7.36 ± 1.71	6.92 ± 0.05	6.80 ± 0.50	11.60 ± 0.60
Slc22a8 (Oat3)		1.25 ± 0.24	1.23 ± 0.04			2.13 ± 0.49
Slc12a2 (Nkcc1)		1.07 ± 0.72	1.28 ± 0.21	2.09 ± 0.24	1.48 ± 0.17	
Slc1a2 (Eaat2)		8.77 ± 1.73	8.85 ± 1.55	12.46 ± 3.88	11.94 ± 1.76	
Slc1a3 (Eaat1)		12.43 ± 0.46	12.99 ± 0.59	9.53 ± 1.50	9.02 ± 2.18	
Slc2a3 (Glut3)		3.89 ± 0.46	3.96 ± 0.58	4.57 ± 1.22	3.64 ± 0.68	
Slc7a1 (Cat1)		2.48 ± 0.31	2.66 ± 1.13	4.42 ± 0.26	3.71 ± 0.15	
Tight junction proteins						
Claudin-5 (Cldn5)		10.09 ± 1.34	9.61 ± 1.27	7.11 ± 1.47	5.76 ± 0.34	7.91 ± 0.90
Cell marker proteins						
Slc2a1 (Glut1)		93.14 ± 13.65	94.11 ± 7.67	73.73 ± 9.21	72.91 ± 1.85	84.00 ± 4.10
Gfap		101.35 ± 41.58	110.11 ± 33.67	114.97 ± 20.90	115.55 ± 14.18	
Syp		11.87 ± 2.89	11.60 ± 2.17	11.69 ± 2.50	10.26 ± 1.48	
Pecam1		4.41 ± 0.29	3.78 ± 0.40	4.88 ± 0.71	4.17 ± 0.78	
γ-gtp (Ggt1)		2.97 ± 0.51	2.72 ± 0.33	2.12 ± 0.35	2.15 ± 0.03	3.07 ± 0.56
Receptors						
Tfrc		5.46 ± 0.97	6.14 ± 1.70	5.89 ± 1.06	5.69 ± 0.52	6.74 ± 0.39
Lrp1		0.98 ± 0.34	0.81 ± 0.21	0.68 ± 0.07	0.68 ± 0.16	1.09 ± 0.14

ABC, ATP-binding cassette; SLC, solute carrier.

^aQuantification values used QconCAT-derived Atp1a1 and Abcb1 abundances as a reference for measurement of protein expression using Progenesis and Maxquant data. Analysis was based on the intensities of peptides from standard and target proteins as shown in Table S2.

^bAtp1a1 is a plasma membrane marker.

^cLiterature values are taken from quantitative proteomic data reported by Hoshi *et al.* (2013).

^dThe reported literature value represents Atp1a subunits $\alpha 1$, $\alpha 2$, and $\alpha 3$ and not exclusively Atp1a1. The quantified protein in this study is Atp1a subunit $\alpha 1$.

described (Achour *et al.* 2017) at 0.06 fmol of peptide on column (translating to protein abundance of 0.1 fmol/μg protein).

Neurovascular unit cell markers were quantified to verify the isolation of microvessels; endothelial cell markers,

glucose transporter 1 (Slc2a1/Glut1), and platelet endothelial cell adhesion molecule (Pecam1), were quantified. The measured abundance of these markers at the protein level is similar to the abundance values reported in the literature (Hoshi *et al.* 2013). Protein abundance of astrocyte and

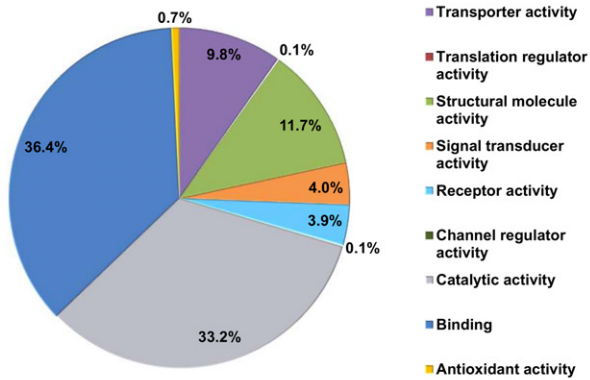
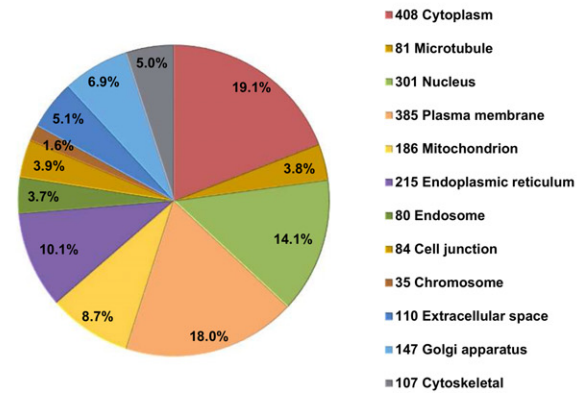
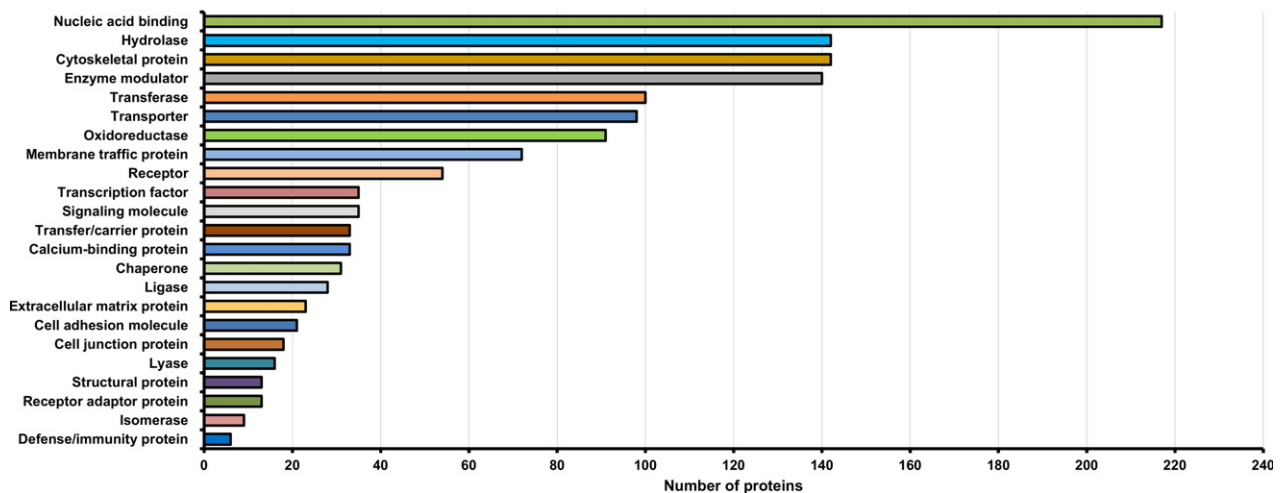
(a) Molecular Function**(b) Cellular Component****(c) Protein class**

Fig. 5 The molecular function, subcellular localization, and protein class of identified proteins; (a) pie chart representing the proportions of identified proteins associated with a specific molecular function (1480 proteins); (b) percentage distribution of proteins from different components of rat brain cells (1980 proteins), assigned by aligning protein

identifiers in the generated dataset against UniProtKB database. The total number (2139 entries) does not match the number of proteins identified as many proteins have more than one subcellular location; and (c) the number of proteins identified in a particular protein class according to the PANTHER classification system.

neuron cell markers (Gfap and Syp) was relatively high, indicating a level of contamination even after optimization of the isolation process (Fig. 6a).

Measurement of Atp1a1 protein abundance contributed to the assessment of plasma membrane transporters; this is an abluminal membrane marker used as a quality control protein along with luminal membrane marker gamma-glutamyl transpeptidase (γ -gtp/Ggt1). LC-MS/MS proteomic data were used to quantify six ABC transporters as shown in Fig. 6(b). The drug transporter Abcb1 (P-gp/Mdr1) exhibited the highest abundance, fivefold higher than Abcg2 and ninefold higher than Abcc4. Furthermore, label-free measurement of Abcb9 and Abcd3 abundance is reported for the first time in this study. Out of 44 solute carrier transporters identified (Table S6), 12 transporters were measured using

label-free quantification (Fig. 6c). Among these transporters, Slco1a4, Slc4a1, Slc25a5, Slc12a2, Slc1a2, Slc1a3, Slc2a3, and Slc7a1 are quantified for the first time in this work. Glucose transporter 1 (Slc2a1) showed the highest measured abundance among the quantified SLC transporters followed by ADP/ATP carrier protein 2 (Slc25a5/Ant2), excitatory amino acid transporter 2 (Slc1a2/Eaat2), and excitatory amino acid transporter 1 (Slc1a3/Eaat1). Other proteins were also measured, including the uptake transporter Slco1a4/Oatp1a4, large neutral amino acids transporter 1 (Slc7a5/Lat1), monocarboxylate transporter 1 (Mct1), cationic amino acid transporter 1 (Slc7a1/Cat1), and glucose transporter 3 (Slc2a3/Glut3). Quantified receptors included transferrin receptor 1 (Tfrc) and low-density lipoprotein receptor-related protein 1 (Lrp1).

Table 3 List of novel transporters identified in rat brain microvessels

Protein	Accession code	Protein score	Mass (Da)	Sequence coverage (%)	Number of peptides	Number of unique peptides	Number of peptides	z	Peptide score	Peptide expected value	Sequence	Type of peptide ^b	Modification
Abca13	D4A885	94	495 469	3	4	4	407.72	+2	23.17	0.0067	NPNDLLK	Unique	Deamidated (N)
							453.74	+2	13.62	0.053	FLNIQNR	Unique	Deamidated (N)
							458.27	+2	19.71	0.53 ^a	ANIEILSR	Unique	-
							410.25	+2	13.52	0.55 ^a	DIALFLK	Unique	-
Slc14a1	P97689	40	42 949	1	2	454.24	+2	16.41	0.049	EFANWLK	Unique	-	
						463.26	+2	23.47	0.039	IFYLQNK	Unique	-	
Slc25a12	F1LX07	480	72 270	19.2	13	787.87	+2	77.70	8.6E-08	AGQTTYSGVIDCFR	Unique	-	
						419.25	+2	42.91	1.2E-4	FGLYLPK	Unique	-	
						667.90	+2	17.67	0.022	GLIPLIGVAPEK	Unique	-	
						620.82	+2	44.90	6.2E-05	GTGSVVGELMYK	Unique	-	
						970.04	+2	90.62	3.2E-09	IAPLAEGALPYNLAEQLR	Unique	-	
						678.40	+2	59.98	6.8E-08	IVQLLAGVADQTK	Unique	-	
						491.27	+2	44.60	6.3E-04	IYSTLAGTR	Unique	-	
						618.33	+2	62.66	2.1E-05	LATATFAGIENK	Unique	-	
						621.34	+2	33.13	0.0038	LQVAGEITGPR	Razor	-	
						465.77	+2	49.72	9.6E-05	LTLADIER	Unique	-	
						482.27	+2	58.18	6.4E-05	LTVNDFVR	Razor	-	
Slc25a13	F1LZW6	64	54 293	4.1	3	723.89	+2	58.84	1.9E-05	PIWLQIAESAYR	Unique	-	
						747.86	+2	55.10	6.8E-06	YLGLYNDPNSNPK	Unique	-	
						667.90	+2	17.67	0.022	GLLPQLLGVAPEK	Unique	-	
						621.34	+2	33.13	0.0038	LQVAGEITGPR	Razor	-	
						482.27	+2	58.18	6.4E-05	LTVNDFVR	Razor	-	
						656.88	+2	14.27	0.046	GAAVNLTVTPEK	Razor	-	
Slc25a22	Q5FVG4	102	25 080	10.5	3	852.37	+2	88.82	4.7E-09	GVNEDTYSGFLLDCAR	Unique	-	
						555.24	+2	17.20	0.024	SEGYFGMYR	Unique	-	
						567.77	+2	17.94	0.021	FWAYEQYK	Unique	-	
						529.75	+2	51.12	1.2E-04	LDFFEFMK	Unique	-	
						755.37	+3	25.17	0.0044	MQAQATTEGAPQLSMVGLFQR	Unique	-	
						599.85	+2	19.35	0.015	QLLAGGVAGVSR	Unique	-	
Slc25a24	B1WCG67	92	53 085	14.5	6	514.75	+2	14.46	0.044	SMNIFGGFR	Unique	-	
						572.28	+2	22.80	0.0082	SYWLDNFAK	Unique	-	
						730.85	+2	36.58	5.6E-04	PLAGTDDSVVSEDR	Unique	-	
						472.28	+2	40.17	0.0043	LLVEDLNK	Unique	-	
Slc39a10	D4A517	79	95 046	1	2	495.74	+2	42.39	1.1E-04	FPYLCYK	Razor	-	
						587.30	+2	40.59	2.5E-04	FYLYPNISR	Unique	Deamidated (N)	

(continued)

Table 3. (continued)

Protein	Accession code	Protein score	Mass (Da)	Sequence coverage (%)	Number of peptides	Number of unique peptides	Precursor m/z	z	Peptide score	Peptide expected value	Sequence	Type of peptide ^b	Modification
Slc6a1	Q01728	38	108 185	3.8	3	3	758.74	+3	30.49	0.003	EIEQLIELANYQVLSQQQK	Unique	-
							452.27	+2	32.08	9.8E-04	GNVLPYK	Unique	-
							949.48	+2	13.68	0.052	GVILPIWEPQDPSFGDK	Unique	-
Slc6a7	P28573	75	59 020	2.5	1	1	742.36	+2	75.29	7.6E-04	PAIDWGPSLEENR	Unique	-

^aPeptides with high expectation values (> 0.05) and/or low scores (< 15) were accepted as supporting evidence only when other unique peptides with high scores and low expectation values were available for the same protein.

^bUnique peptides were used for identification and quantification; razor peptides (unique for but shared between a subset of proteins, e.g., a subfamily) were used as supporting evidence for identification only.

Discussion

The quantification of BBB transporters is important not only in pharmacokinetic studies to understand the disposition of drugs and their metabolites into the CNS and to elucidate drug–drug interactions (Giacomini *et al.* 2010; Kalvass *et al.* 2013), but also as a critical step in the interpretation of safety-related issues in animals and their extrapolation to humans (Hamon *et al.* 2015). The development of PBPK models for psychoactive drugs (and other drugs that can penetrate the BBB), particularly when they are subject to active uptake or efflux, is therefore dependent on robust and reliable measurement of the abundances of BBB transporters in humans as well as animal species used in pre-clinical studies (Ball *et al.* 2014; Gaohua *et al.* 2016). Recent applications of such PBPK models also highlight their potential in assessing the needs of subpopulations, which are not fully explored in clinical studies (e.g., pediatrics, brain cancer patients) as reported previously (Spanakis *et al.* 2016; Kalluri *et al.* 2017; Donovan *et al.* 2018).

In this study, we were able to optimize the isolation of rat brain microvessels using a systematic assessment of various combinations of density gradient centrifugation and filtration. Throughout the experiments, we applied quality control steps in sample preparation, at multiple levels using RNA expression to assess the enrichment and purity of microvessels. Additional quality controls included comparing the performance of in-solution sample preparation with FASP for proteomic analysis, assessing the required amount of sample analyzed, and comparing reproducibility of detection of peptides in replicates.

In addition to assessing enrichment of endothelial cells, the purity of microvessels was assessed by the gradual decrease in expression of marker genes for astrocytes, and neurons, in line with published literature (Yousif *et al.* 2007; Dauchy *et al.* 2008). These markers were also detected in isolated samples by proteomic analysis, indicating some level of contamination of microvessels. The contribution of astrocytes and pericytes to the composition of the BBB is still unclear. Therefore, even though transporters relevant to BBB drug traffic are localized on the membrane of endothelial cells, the role of these transporters in other cell types cannot be excluded.

Factors considered to improve the isolation methodology are shown in Table 1. The use of protease inhibitors throughout the isolation was adopted to inhibit degradation of protein, and sterile disposable cell strainers were used instead of a nylon mesh sheet to remove cell debris and decrease the possibility of contamination. In addition, empirical adjustment of centrifugation speeds improved the separation of microvessels from the myelin layer. The improvement in isolation methodology is reflected in the increased numbers of peptides observed in sample 3S versus 1S (Fig. 4a). Further optimization was then achieved at the

level of sample preparation, where FASP led to the identification of a larger number of peptides and transporters compared to in-solution sample preparation (Fig. 4a and b). The combination of deoxycholate and urea used for FASP has been reported to increase digestion efficiency for both cytosolic and membrane proteins, whereas the use of deoxycholate only in the in-solution preparation enhances digestion of membrane proteins (Balogh *et al.* 2013). In addition, sample loss during in-solution digestion can occur because of precipitation of deoxycholate to collect peptides in the supernatant.

The optimization process enabled the identification of nearly 2000 proteins in rat brain microvessels using a combination of LC–MS/MS and bioinformatic approaches and a rigorous razor. Plasma membrane proteins constituted approximately 18% of all identified proteins using Progenesis, and proteins with transport activity represented nearly 10% of identified proteins with known function. We focused on the identification of membrane-associated proteins with function in molecular transport, with a total of 44 SLC and 8 ABC transporters. These results are comparable to previously reported LC–MS/MS proteomic data on rat brain microvessels (Gomez-Zepeda *et al.* 2017), where 1640 proteins were identified, including 44 SLC and 6 ABC transporters. Although the two studies identified similar numbers of proteins and transporters, the two datasets were rather complementary, where the overlap was 30 SLC and 4 ABC transporters. We note, however, that the number of transporters reported by Gomez-Zepeda *et al.* was based simply on output from the Mascot search engine; we further subjected each transporter peptide to a BLAST search (basic local alignment search tool) against the UniProt database, and this resulted in a reduction in the number of SLC transporters from 58 to 44 and the number of ABC transporters from 12 to 8 (Table S6). Using this approach, we were able to identify 10 transporters (Table 3) for the first time in rat brain microvessels (Abca13, Slc14a1, Slc25a12, Slc25a13, Slc25a22, Slc25a24, Slc39a10, Slc6a6, Slc6a7, and Slc8a1), which are involved in physiological functions related to maintaining brain homeostasis.

A normal limitation of untargeted proteomics and lack of enrichment of target proteins in a plasma membrane fraction is signal suppression and underestimation of measurements due to matrix effects (Wegler *et al.* 2017). Our approach combines the advantages of targeted and global analyses to achieve reliable quantification, as previously advocated (Al Feteisi *et al.* 2015b) and, where literature values are available, the dataset shows good agreement. The use of data-dependent acquisition in this report was mainly because of availability of mass spectrometers capable of such technique and access to corresponding data analysis tools, with advantages such as broad coverage at the MS/MS level and ease of analysis (Gillette and Carr 2013). However, owing to sampling of peptides based on intensity, this

technique suffers from high variability and compromised reproducibility when low abundance proteins are quantified. Data-independent acquisition has recently been suggested to overcome such a limitation, but this technique generates highly complex data and it still requires development of robust data analysis methods (Doerr 2015). Recent improvements in resolution, accuracy, and speed of mass spectrometers improved the reproducibility of data-dependent methods, which remain the standard approach in proteomic research.

The adopted quantitative strategy enabled quantification of 1276 proteins. Atp1a1, Abcb1, and Abcc4 were quantified using QconCAT-based targeted quantitative proteomics. The main purpose of using targeted quantification was to quantify the reference plasma membrane marker (Atp1a1) for label-free analysis. Further quantification using label-free methodology generated equivalent abundance values for Abcb1 and Abcc4. The label-free quantification was confirmed using a second reference protein, Abcb1. Although the plasma membrane marker (Atp1a1) was preferred as a standard, it was reassuring that all the quantifications were the same to within 1.5-fold when Abcb1 was used. From a translational perspective, the two sets of values would be considered interchangeable (Achour *et al.* 2018). Where quantification was achieved using Progenesis software, there was agreement to within 1.2-fold.

In the rat BBB dataset, Abcb1 was the most abundant ABC transporter, in agreement with published literature (Hoshi *et al.* 2013). In contrast, Abcg2 is reported to be more abundant than Abcb1 in human and cynomolgus monkey, which indicates inter-species differences as a result of Abcb1 being encoded by two genes (Abcb1a/b) in rodents compared to only one in humans (Ito *et al.* 2011; Shawahna *et al.* 2011; Uchida *et al.* 2011). This suggests the possibility that P-gp has a higher activity in rat, which can be important in extrapolation to human dosing, especially with drugs that are substrates of both P-gp and Bcrp as potential drug–drug interaction prediction may not be accurate. For example, studies on P-gp and Bcrp activity using knockout mice and dual pharmacological inhibition in wild-type mice have shown greatly increased brain accumulation of the anticancer drug, gefitinib, which is believed to be effluxed across the BBB by P-gp and Bcrp transporters (Agarwal *et al.* 2010). However, this may not translate to the clinical setting, as drug–drug interactions because of inhibition of brain efflux transporters are very rare in humans compared to animal models (Kalvass *et al.* 2013). Therefore, these inter-species differences raise some concerns over the reliability of extrapolating animal data from pre-clinical studies to predict human brain drug distribution. Abcc4 was the main Mrp protein detected in rat brain microvessels, which is similar to previously reported findings (Hoshi *et al.* 2013), with relevance to the protective role of Mrp proteins (including Mrp4 and Mrp9) by limiting BBB penetration of neurotoxins

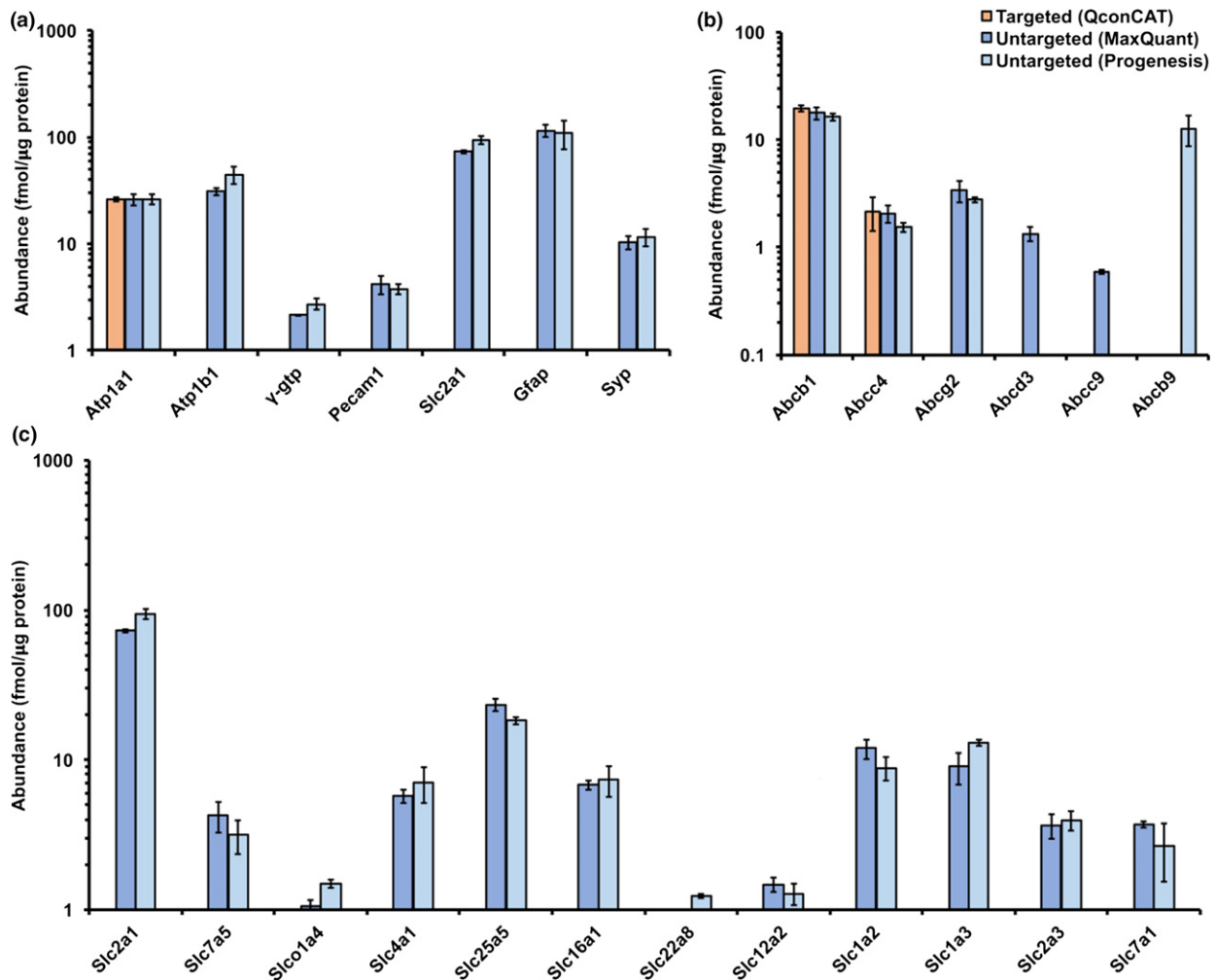


Fig. 6 Abundances of identified proteins using targeted (QconCAT) and untargeted (MaxQuant, Progenesis) methods; (a) comparison of abundances of plasma membrane markers and neurovascular unit-specific cell markers; (b) abundances of ABC transporters; and (c) abundances of SLC transporters; the data represent mean values \pm SD ($n = 4$ replicates) of the pooled sample 4F.

and chemotherapeutic drugs (Leggas *et al.* 2004; Nelson *et al.* 2015). Another role of Mrp9 (Abbc9) is its function in neuronal excitability by regulating potassium channels in neurons (Nelson *et al.* 2015). Furthermore, the label-free quantification strategy was able to measure Abcb9 and Abcd3 for the first time. Although the role of Abcb9 is yet to be elucidated, this transporter appears to be related to lysosomal function (Zhang *et al.* 2000). Abcd3, along with other Abcd transporters which function in the peroxisomal membrane, is involved in fatty acid homeostasis (Baker *et al.* 2015).

In addition to ABC transporters, 44 SLC transporters were identified, of which 27 were quantified. Solute carrier transporters play an important role in delivering nutrients across the BBB. These include glucose (Glut1, Glut3) and amino acid (Cat1, Lat1, Eaat1, and Eaat2) transporters, which are involved in brain homeostasis and can therefore be implicated in several

disease states. Glut1 has the highest transporter expression in the BBB and is localized on both the luminal and abluminal sides of the barrier (Ohtsuki and Terasaki 2007). Amino acid transporters, Cat1, Eaat1, and Eaat2, are quantified for the first time. The combined label-free/targeted strategy was also used to measure bidirectional drug transporters Slco1a4 (Oatp1a4) and Slc22a8 (Oat3). In human brain microvessels, both SLCO1A4 and SLC22A8 were reported to be below the limit of quantification (Uchida *et al.* 2011). Rat Slco1a4 is involved in the transport of digoxin, opioids, and organic anions across the BBB (Ohtsuki and Terasaki 2007), while Slc22a8 plays a role in the efflux of oseltamivir and the dopamine metabolite, homovanillic acid (Uchida *et al.* 2014). Slc16a1 (Mct1) transports lactates and ketones as an alternative source of energy to the brain (Abbott *et al.* 2010; Ohtsuki *et al.* 2014). Lat1 is an endogenous transporter for large neutral amino acids and its ability to transport substrates to the brain was previously

utilized to deliver drugs, such as L-DOPA and gabapentin, into the brain (Gomes and Soares-Da-Silva 1999; Dickens *et al.* 2013). Cross-species differences have been reported in the expression of Lat1, with higher levels in rodents than in humans (Uchida *et al.* 2011). The quantitative strategy adopted in this study also allowed the measurement of two receptors, low-density lipoprotein receptor-related protein (Lrp1) and transferrin receptor 1 (Tfrc), with abundances similar to those previously reported (Hoshi *et al.* 2013). Characterization of brain receptors can be useful in understanding the pharmacodynamics of psychoactive drugs and the implications of neurodegenerative diseases, including dementia.

In conclusion, this study reports successful optimization of brain microvessel isolation and sample preparation. A substantial number of BBB proteins, including transporters, were identified and quantified using a combination of proteomic approaches and bioinformatics tools. Although differences in proteomic methods can result in discrepancies in reported end-point abundances (Wegler *et al.* 2017), optimization and standardization, such as this work, should lead to reliable quantification and subsequently valid pharmacokinetic/pharmacodynamic conclusions (Harwood *et al.* 2016; Rostami-Hodjegan 2017). Inter-species differences between rats and humans are highlighted, in line with published literature. These differences reiterate the challenges of using pre-clinical models for CNS drug pharmacokinetic/pharmacodynamic studies, which may necessitate avoiding direct extrapolation and employing model-based translation (Fig. 1). Considering neurotoxic effects of psychoactive and non-psychoactive drugs that can cross the BBB is dependent on elucidating transporter abundance and activity, which are key to bridging the gap in translation from animal models to human clinical practice. Other implications include stratification of patients with different susceptibilities and requirements for dose adjustment as demonstrated recently by examples in pediatrics in relation to hepatic transporters (Elmorsi *et al.* 2016).

Acknowledgments and conflict of interest disclosure

The authors thank the Biological Mass Spectrometry Core Facility (Bio-MS), University of Manchester, for access to LC-MS/MS instrumentation. This study was partly supported by the Simcyp (Certara) Grant and Partnership Scheme (GPS 2014/15). The authors report no conflict of interest.

All experiments were conducted in compliance with the ARRIVE guidelines.

Supporting information

Additional supplemental material may be found online in the Supporting Information section at the end of the article.

Figure S1. Correlation analysis showing agreement between targeted QconCAT measurements and two intensity-based label-free analysis approaches (MaxQuant and Progenesis) that used Atp1a1 abundance as a reference.

Table S1. Percentage identical peptides and proteins between replicates and between software packages.

Table S2. Summary of quantification of each peptide using two different software packages.

Table S3. Razor applied to peptide data.

Table S4. Protein identification using Progenesis.

Table S5. Protein quantification using Progenesis data.

Table S6. List of peptides used in the identification of transporters in rat brain microvessels (44 SLC transporters and 8 ABC transporters).

Appendix S1. Supplementary Materials and methods.

References

- Abbott N. J., Rönnbäck L. and Hansson E. (2006) Astrocyte-endothelial interactions at the blood-brain barrier. *Nat. Rev. Neurosci.* **7**, 41–53.
- Abbott N. J., Patabendige A. A. K., Dolman D. E. M., Yusof S. R. and Begley D. J. (2010) Structure and function of the blood-brain barrier. *Neurobiol. Dis.* **37**, 13–25.
- Abduljalil K., Johnson T. N. and Rostami-Hodjegan A. (2018) Fetal physiologically based pharmacokinetic models: systems information on fetal biometry and gross composition. *Clin. Pharmacokinet.* In press <https://doi.org/10.1007/s40262-017-0618-1>.
- Achour B., Russell M. R., Barber J. and Rostami-Hodjegan A. (2014) Simultaneous quantification of the abundance of several cytochrome P450 and uridine 5'-diphospho-glucuronosyltransferase enzymes in human liver microsomes using multiplexed targeted proteomics. *Drug Metab. Dispos.* **42**, 500–510.
- Achour B., Al-Majdoub Z. M., Al Feteisi H., Elmorsi Y., Rostami-Hodjegan A. and Barber J. (2015) Ten years of QconCATs: Application of multiplexed quantification to small medically relevant proteomes. *Int. J. Mass Spectrom.* **391**, 93–104.
- Achour B., Al Feteisi H., Lanucara F., Rostami-Hodjegan A. and Barber J. (2017) Global proteomic analysis of human liver microsomes: rapid characterization and quantification of hepatic drug-metabolizing enzymes. *Drug Metab. Dispos.* **45**, 666–675.
- Achour B., Dantonio A., Niosi M., Novak J. J., Al-Majdoub Z. M., Goosen T. C., Rostami-Hodjegan A. and Barber J. (2018) Data generated by quantitative liquid chromatography-mass spectrometry proteomics are only the start and not the endpoint: optimization of quantitative concatemer-based measurement of hepatic uridine-5'-diphosphate-glucuronosyltransferase enzymes with reference to catalytic activity. *Drug Metab. Dispos.* **46**, 805–812. In press.
- Agarwal N., Lippmann E. S. and Shusta E. V. (2010) Identification and expression profiling of blood-brain barrier membrane proteins. *J. Neurochem.* **112**, 625–635.
- Al Feteisi H., Achour B., Barber J. and Rostami-Hodjegan A. (2015a) Choice of LC-MS methods for the absolute quantification of drug-metabolizing enzymes and transporters in human tissue: a comparative cost analysis. *AAPS J* **17**, 438–446.
- Al Feteisi H., Achour B., Rostami-Hodjegan A. and Barber J. (2015b) Translational value of liquid chromatography coupled with tandem mass spectrometry-based quantitative proteomics for in vitro – in vivo extrapolation of drug metabolism and transport and

- considerations in selecting appropriate techniques. *Expert Opin. Drug Metab. Toxicol.* **11**, 1357–1369.
- Baker A., Carrier D. J., Schaedler T., Waterham H. R., van Roermund C. W. and Theodoulou F. L. (2015) Peroxisomal ABC transporters: functions and mechanism. *Biochem. Soc. Trans.* **43**, 959–965.
- Ball K., Bouzom F., Scherrmann J. M., Walther B. and Declèves X. (2014) Comparing translational population-PBPK modelling of brain microdialysis with bottom-up prediction of brain-to-plasma distribution in rat and human. *Biopharm. Drug Dispos.* **35**, 485–499.
- Balogh L. M., Kimoto E., Chupka J., Zhang H. and Lai Y. (2013) Membrane protein quantification by peptide-based mass spectrometry approaches: studies on the organic anion-transporting polypeptide family. *J. Proteomics Bioinform.* **6**, 229–236.
- Cardoso F. L., Brites D. and Brito M. A. (2010) Looking at the blood–brain barrier: molecular anatomy and possible investigation approaches. *Brain Res. Rev.* **64**, 328–363.
- Couto N., Barber J. and Gaskell S. J. (2011) Matrix-assisted laser desorption/ionisation mass spectrometric response factors of peptides generated using different proteolytic enzymes. *J. Mass Spectrom.* **46**, 1233–1240.
- Couto N., Wright P. and Barber J. (unpublished) Electrospray ionization mass spectrometry response of peptides generated by different proteolytic enzymes: a case for alternatives to trypsin in proteomics. (Submitted for publication).
- Dauchy S., Dutheil F., Weaver R. J., Chassoux F., Daumas-Duport C., Couraud P.-O., Scherrmann J.-M., Waziers I. and De Declèves X. (2008) ABC transporters, cytochromes P450 and their main transcription factors: expression at the human blood–brain barrier. *J. Neurochem.* **107**, 1518–1528.
- Dickens D., Webb S. D., Antonyuk S., Giannoudis A., Owen A., Rädisch S., Hasnain S. S. and Pirmohamed M. (2013) Transport of gabapentin by LAT1 (SLC7A5). *Biochem. Pharmacol.* **85**, 1672–1683.
- Doerr A. (2015) DIA mass spectrometry. *Nat. Methods* **12**, 35.
- Donovan M., Abduljalil K., Cryan J., Boylan G. and Griffin B. (2018) Application of a physiologically-based pharmacokinetic model for the prediction of bumetanide plasma and brain concentrations in the neonate. *Biopharm. Drug Dispos.* **39**, 125–134.
- Elmorsi Y., Barber J. and Rostami-Hodjegan A. (2016) Ontogeny of hepatic drug transporters and relevance to drugs used in pediatrics. *Drug Metab. Dispos.* **44**, 992–998.
- Erickson M. A. and Banks W. A. (2013) Blood–brain barrier dysfunction as a cause and consequence of Alzheimer's disease. *J. Cereb. Blood Flow Metab.* **33**, 1500–1513.
- Gaohua L., Neuhoff S., Johnson T. N., Rostami-Hodjegan A. and Jamei M. (2016) Development of a permeability-limited model of the human brain and cerebrospinal fluid (CSF) to integrate known physiological and biological knowledge: estimating time varying CSF drug concentrations and their variability using in vitro data. *Drug Metab. Pharmacokinet.* **31**, 224–233.
- Giacomini K. M., Huang S.-M., Tweedie D. J. *et al.* (2010) Membrane transporters in drug development. *Nat. Rev. Drug Discov.* **9**, 215–236.
- Gillette M. A. and Carr S. A. (2013) Quantitative analysis of peptides and proteins in biomedicine by targeted mass spectrometry. *Nat. Methods* **10**, 28–34.
- Golden P. L. and Pollack G. M. (2003) Blood–brain barrier efflux transport. *J. Pharm. Sci.* **92**, 1739–1753.
- Gomes P. and Soares-da-Silva P. (1999) L-DOPA transport properties in an immortalised cell line of rat capillary cerebral endothelial cells, RBE 4. *Brain Res.* **829**, 43–50.
- Gomez-Zepeda D., Chaves C., Taghi M. *et al.* (2017) Targeted unlabeled multiple reaction monitoring analysis of cell markers for the study of sample heterogeneity in isolated rat brain cortical microvessels. *J. Neurochem.* **142**, 597–609.
- Hamon J., Renner M., Jamei M., Lukas A., Kopp-Schneider A. and Bois F. Y. (2015) Quantitative in vitro to in vivo extrapolation of tissues toxicity. *Toxicol. In Vitro* **30**, 203–216.
- Harwood M. D., Achour B., Russell M. R., Carlson G. L., Warhurst G. and Rostami-Hodjegan A. (2015) Application of an LC–MS/MS method for the simultaneous quantification of human intestinal transporter proteins absolute abundance using a QconCAT technique. *J. Pharm. Biomed. Anal.* **110**, 27–33.
- Harwood M. D., Achour B., Neuhoff S., Russell M. R., Carlson G., Warhurst G. and Rostami-Hodjegan A. (2016) In vitro-in vivo extrapolation scaling factors for intestinal p-glycoprotein and breast cancer resistance protein: Part II. The impact of cross-laboratory variations of intestinal transporter relative expression factors on predicted drug disposition. *Drug Metab. Dispos.* **44**, 476–480.
- Hoshi Y., Uchida Y., Tachikawa M., Inoue T., Ohtsuki S. and Terasaki T. (2013) Quantitative Atlas of blood–brain barrier transporters, receptors, and tight junction proteins in rats and common marmoset. *J. Pharm. Sci.* **102**, 3343–3355.
- Ito K., Uchida Y., Ohtsuki S., Aizawa S., Kawakami H., Katsukura Y., Kamiie J. and Terasaki T. (2011) Quantitative membrane protein expression at the blood–brain barrier of adult and younger cynomolgus monkeys. *J. Pharm. Sci.* **100**, 3939–3950.
- Kalluri H. V., Zhang H., Caritis S. N. and Venkataraman R. (2017) A physiologically based pharmacokinetic modelling approach to predict buprenorphine pharmacokinetics following intravenous and sublingual administration. *Br. J. Clin. Pharmacol.* **83**, 2458–2473.
- Kalvass J. C., Polli J. W., Bourdet D. L., Feng B., Huang S.-M., Liu X., Smith Q. R., Zhang L. K. and Zamek-Gliszczyński M. J. (2013) Why clinical modulation of efflux transport at the human blood–brain barrier is unlikely: the ITC evidence-based position. *Clin. Pharmacol. Ther.* **94**, 80–94.
- Keifer J. and Summers C. H. (2016) Putting the “Biology” back into “Neurobiology”: the strength of diversity in animal model systems for neuroscience research. *Front. Syst. Neurosci.* **10**, 1–9.
- Leggas M., Adachi M., Scheffer G. *et al.* (2004) MRP4 confers resistance to topotecan and protects the brain from chemotherapy. *Mol. Cell. Biol.* **24**, 7612–7621.
- Masuda T., Tomita M. and Ishihama Y. (2008) Phase transfer surfactant-aided trypsin digestion for membrane proteome analysis Phase Transfer Surfactant-Aided Trypsin Digestion for Membrane. *J. Proteome Res.* **7**, 731–740.
- Mi H., Muruganujan A., Casagrande J. T. and Thomas P. D. (2013) Large-scale gene function analysis with the PANTHER classification system. *Nat. Protoc.* **8**, 1551–1566.
- Nelson P. T., Jicha G. A., Wang W.-X., Ighodaro E., Artiushin S., Nichols C. G. and Fardo D. W. (2015) ABC9/SUR2 in the brain: implications for hippocampal sclerosis of aging and a potential therapeutic target. *Ageing Res. Rev.* **24**, 111–125.
- Ohtsuki S. and Terasaki T. (2007) Contribution of carrier-mediated transport systems to the blood–brain barrier as a supporting and protecting interface for the brain; importance for CNS drug discovery and development. *Pharm. Res.* **24**, 1745–1758.
- Ohtsuki S., Hirayama M., Ito S., Uchida Y., Tachikawa M. and Terasaki T. (2014) Quantitative targeted proteomics for understanding the blood–brain barrier: towards pharmacoproteomics. *Exp. Rev. Proteomics* **11**, 303–313.
- Pardridge W. M., Eisenberg J. and Yamada T. (1985) Rapid sequestration and degradation of somatostatin analogues by isolated brain microvessels. *J. Neurochem.* **44**, 1178–1184.
- Persidsky Y., Ramirez S. H., Haorah J. and Kanmogne G. D. (2006) Blood–brain barrier: structural components and function under

- physiologic and pathologic conditions. *J. Neuroimmune Pharmacol.* **1**, 223–236.
- Rostami-Hodjegan A. (2017) Reverse translation in PBPK and QSP: going backwards in order to go forward with confidence. *Clin. Pharmacol. Ther.* **103**, 224–232.
- Russell M. R., Achour B., Mckenzie E. A., Lopez R., Harwood M. D., Rostami-Hodjegan A. and Barber J. (2013) Alternative fusion protein strategies to express recalcitrant QconCAT proteins for quantitative proteomics of human drug metabolizing enzymes and transporters. *J. Proteome Res.* **12**, 5934–5942.
- Silva J. C., Gorenstein M. V., Li G. Z., Vissers J. P. and Geromanos S. J. (2006) Absolute quantification of proteins by LCMSE a virtue of parallel MS acquisition. *Mol. Cell Proteomics* **5**, 144–156.
- Schinkel A. H. and Jonker J. W. (2012) Mammalian drug efflux transporters of the ATP binding cassette (ABC) family: an overview. *Adv. Drug Deliv. Rev.* **64**, 138–153.
- Scotcher D., Jones C., Posada M., Galetin A. and Rostami-Hodjegan A. (2016) Key to opening kidney for in vitro-in vivo extrapolation entrance in health and disease: Part II: mechanistic models and in vitro-in vivo extrapolation. *AAPS J* **18**, 1082–1094.
- Shawahna R., Uchida Y., Declèves X. *et al.* (2011) Transcriptomic and quantitative proteomic analysis of transporters and drug metabolizing enzymes in freshly isolated human brain microvessels. *Mol. Pharm.* **8**, 1332–1341.
- Sobotka T. J., Ekelman K. B., Slikker W., Raffaele K. and Hattan D. G. (1996) Food and Drug Administration proposed guidelines for neurotoxicological testing of food chemicals. *Neurotoxicology* **17**, 825–836.
- Spanakis M., Kontopodis E., Van Cauter S., Sakkalis V. and Marias K. (2016) Assessment of DCE-MRI parameters for brain tumors through implementation of physiologically-based pharmacokinetic model approaches for Gd-DOTA. *J. Pharmacokinetic Pharmacodyn.* **43**, 529–547.
- Uchida Y., Ohtsuki S., Katsukura Y., Ikeda C., Suzuki T., Kamiie J. and Terasaki T. (2011) Quantitative targeted absolute proteomics of human blood-brain barrier transporters and receptors. *J. Neurochem.* **117**, 333–345.
- Uchida Y., Tachikawa M., Ohtsuki S. and Terasaki T. (2014) Blood–brain barrier (BBB) pharmacoproteomics: a new research field opened up by quantitative targeted absolute proteomics (QTAP), in *Drug Delivery to Brain* (Hammarlund-Udenaes M., de Lange E. C. M. and Thorne R. G., eds), Vol. **10**, pp. 63–100. Springer, New York.
- Wegler C., Gaugaz F. Z., Andersson T. B. *et al.* (2017) Variability in mass spectrometry-based quantification of clinically relevant drug transporters and drug metabolizing enzymes. *Mol. Pharm.* **14**, 3142–3151.
- Wiśniewski J. R., Zougman A., Nagaraj N. and Mann M. (2009) Universal sample preparation method for proteome analysis. *Nat. Methods* **6**, 359–362.
- Yousif S., Marie-Claire C., Roux F., Scherrmann J.-M. and Declèves X. (2007) Expression of drug transporters at the blood–brain barrier using an optimized isolated rat brain microvessel strategy. *Brain Res.* **1134**, 1–11.
- Zhang F., Zhang W., Liu L., Fisher C. L., Hui D., Childs S., Dorovini-Zis K. and Ling V. (2000) Characterization of ABCB9, an ATP binding cassette protein associated with lysosomes. *J. Biol. Chem.* **275**, 23287–23294.
- Zheng W., Aschner M. and Ghersi-Egea J.-F. (2003) Brain barrier systems: a new frontier in metal neurotoxicological research. *Toxicol. Appl. Pharmacol.* **192**, 1–11.